

The Curvature of $F_2^p(x, Q^2)$ as a Probe of Perturbative QCD Evolutions in the small- x Region

Cristian Pisano

Department of Physics and Astronomy, Vrije Universiteit Amsterdam,
De Boelelaan 1081, 1081 HV Amsterdam - The Netherlands

Perturbative NLO and NNLO QCD evolutions of parton distributions are studied, in particular in the (very) small- x region, where they are in very good agreement with all recent precision measurements of $F_2^p(x, Q^2)$. These predictions turn out to be also rather insensitive to the specific choice of the factorization scheme ($\overline{\text{MS}}$ or DIS). A characteristic feature of perturbative QCD evolutions is a *positive* curvature of F_2^p which increases as x decreases. This perturbatively stable prediction provides a sensitive test of the range of validity of perturbative QCD.

The curvature of DIS structure functions like $F_2^p(x, Q^2)$, i.e., its second derivative with respect to the photon's virtuality Q^2 at fixed values of x , plays a decisive role in probing the range of validity of perturbative QCD evolutions of parton distributions in the small- x region. This has been observed recently [1, 2, 3, 4] and it was demonstrated that NLO($\overline{\text{MS}}$) evolutions imply a *positive* curvature which increases as x decreases. Such rather unique predictions provide a check of the range of validity of perturbative QCD evolutions. However, the curvature is a rather subtle mathematical quantity which a priori may sensitively depend on the theoretical (non)perturbative assumptions made for calculating it. Our main purpose is to study the dependence and stability of the predicted curvature with respect to a different choice of the factorization scheme (DIS versus $\overline{\text{MS}}$) and to the perturbative order of the evolutions by extending the common NLO (2-loop) evolution [3] to the next-to-next-to-leading 3-loop order (NNLO) [4].

The valence $q_v = u_v, d_v$ and sea $w = \bar{q}, g$ distributions underlying $F_2^p(x, Q^2)$ are parametrized at an input scale $Q_0^2 = 1.5 \text{ GeV}^2$ as follows:

$$x q_v(x, Q_0^2) = N_{q_v} x^{a_{q_v}} (1-x)^{b_{q_v}} (1 + c_{q_v} \sqrt{x} + d_{q_v} x + e_{q_v} x^{1.5}) \quad (1)$$

$$x w(x, Q_0^2) = N_w x^{a_w} (1-x)^{b_w} (1 + c_w \sqrt{x} + d_w x) \quad (2)$$

and without loss of generality the strange sea is taken to be $s = \bar{s} = 0.5 \bar{q}$. Notice that we do not consider sea breaking effects ($\bar{u} \neq \bar{d}$, $s \neq \bar{s}$) since the data used, and thus our analysis, are not sensitive to such corrections. The normalizations N_{u_v} and N_{d_v} are fixed by $\int_0^1 u_v dx = 2$ and $\int_0^1 d_v dx = 1$, respectively, and N_g is fixed via $\int_0^1 x(\Sigma + g) dx = 1$. We have performed all Q^2 -evolutions in Mellin n -moment space and used the QCD-PEGASUS program [5] for the NNLO evolutions. For definiteness we work in the fixed flavor factorization scheme, rather than in the variable (massless quark) scheme since the results for F_2^p and its curvature remain essentially unchanged [3].

We have somewhat extended the set of DIS data used in [3] in order to determine the remaining parameters at larger values of x and of the valence distributions. The following data sets have been used: the small- x [6] and large- x [7] H1 F_2^p data; the fixed target BCDMS data [8] for F_2^p and F_2^n using $Q^2 \geq 20 \text{ GeV}^2$ and $W^2 = Q^2(\frac{1}{x} - 1) + m_p^2 \geq 10 \text{ GeV}^2$ cuts, and the proton and deuteron NMC data [9] for $Q^2 \geq 4 \text{ GeV}^2$ and $W^2 \geq 10 \text{ GeV}^2$. This amounts to a total of 740 data points. The required overall normalization factors of

	NNLO($\overline{\text{MS}}$)				NLO($\overline{\text{MS}}$)			
	u_v	d_v	\bar{q}	g	u_v	d_v	\bar{q}	g
N	0.2503	3.6204	0.1196	2.1961	0.4302	0.3959	0.0546	2.3780
a	0.2518	0.9249	-0.1490	-0.0121	0.2859	0.5375	-0.2178	-0.0121
b	3.6287	6.7111	3.7281	6.5144	3.5503	5.7967	3.3107	5.6392
c	4.7636	6.7231	0.6210	2.0917	1.1120	22.495	5.3095	0.8792
d	24.180	-24.238	-1.1350	-3.0894	15.611	-52.702	-5.9049	-1.7714
e	9.0492	30.106	—	—	4.2409	69.763	—	—
χ^2/dof	0.989				0.993			
$\alpha_s(M_Z^2)$	0.112				0.114			

Table 1: Parameter values of the NLO and NNLO QCD fits with the parameters of the input distributions referring to (1) and (2).

the data are 0.98 for BCDMS and 1.0 for NMC. The resulting parameters of the NLO($\overline{\text{MS}}$) and NNLO($\overline{\text{MS}}$) fits are summarized in Table 1.

The quantitative difference between the NLO($\overline{\text{MS}}$) and NLO(DIS) results turns out to be rather small [4]. Therefore we do not consider any further the DIS scheme in NNLO. The present more detailed NLO($\overline{\text{MS}}$) analysis corresponds to $\chi^2/\text{dof} = 715.3/720$ and the results are comparable to our previous ones [3]. Our new NLO(DIS) and NNLO(3-loop) fits are also very similar, corresponding to $\chi^2/\text{dof} = 714.2/720$ and $712.0/720$, respectively. It should be emphasized that the perturbatively stable QCD predictions are in perfect agreement with all recent high-statistics measurements of the Q^2 -dependence of $F_2^p(x, Q^2)$ in the (very) small- x region. Therefore additional model assumptions concerning further resummations of sub-leading small- x logarithms (see, for example, [10]) are not required [11, 12].

Figure 1 shows our gluon input distributions in (1) and Table 1 as obtained in our three different fits, as well as their evolved shapes at $Q^2 = 4.5 \text{ GeV}^2$ in particular in the small- x region. In order to allow for a consistent comparison in the $\overline{\text{MS}}$ scheme, our NLO(DIS) results have been transformed to the $\overline{\text{MS}}$ factorization scheme. Note, however, that the gluon distribution in the DIS scheme is very similar to the one obtained in NLO($\overline{\text{MS}}$) shown in Fig. 1 which holds in particular in the small- x region. This agreement becomes even better for increasing values of Q^2 . This agreement is similar for the sea distributions in the

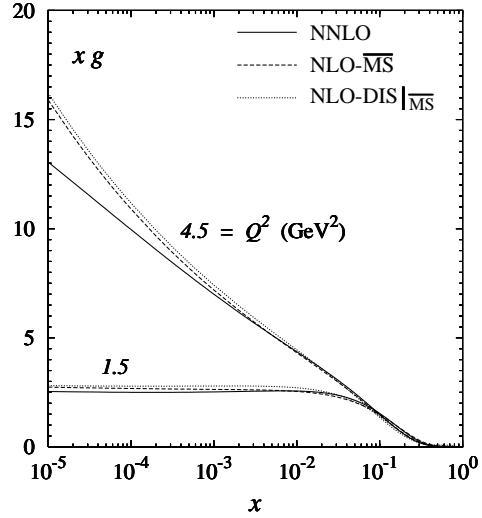


Figure 1: The gluon distributions at the input scale $Q_0^2 = 1.5 \text{ GeV}^2$ and at $Q^2 = 4.5 \text{ GeV}^2$.

small- x region. Only for $x \gtrsim 0.1$ the NLO(DIS) sea density becomes sizeably smaller than the NLO($\overline{\text{MS}}$) one. The NLO results are rather similar but distinctively different from the NNLO ones in the very small- x region at $Q^2 > Q_0^2$. In particular the strong increase of the gluon distribution $xg(x, Q^2)$ as $x \rightarrow 0$ at NLO is somewhat tamed by NNLO 3-loop effects.

Turning now to the curvature of F_2^p we first present in Fig. 2 our results for $F_2^p(x, Q^2)$ at $x = 10^{-4}$, together with a global fit MRST01 NLO result [13], as a function of [2]

$$q = \log_{10} \left(1 + \frac{Q^2}{0.5 \text{ GeV}^2} \right) . \quad (3)$$

This variable has the advantage that most measurements lie along a straight line [2] as indicated by the dotted line in Fig. 2. All our three NLO and NNLO fits give almost the same results which are also very similar [3] to the global CTEQ6M NLO fit [14]. In contrast to all other fits shown in Fig. 2, only the MRST01 parametrization results in a sizeable curvature for F_2^p . More explicitly the curvature can be directly extracted from

$$F_2^p(x, Q^2) = a_0(x) + a_1(x)q + a_2(x)q^2 . \quad (4)$$

The curvature $a_2(x) = \frac{1}{2} \partial_q^2 F_2^p(x, Q^2)$ is evaluated by fitting this expression to the predictions for $F_2^p(x, Q^2)$ at fixed values of x to a (kinematically) given interval of q . In Figure 3 we present $a_2(x)$ which results from experimentally selected q -intervals [2, 3, 4]:

$$\begin{array}{ll} 0.7 \leq q \leq 1.4 & \text{for} \quad 2 \times 10^{-4} < x < 10^{-2} \\ 0.7 \leq q \leq 1.2 & \text{for} \quad 5 \times 10^{-5} < x \leq 2 \times 10^{-4} . \end{array} \quad (5)$$

It should be noticed that the average value of q decreases with decreasing x due to the kinematically more restricted Q^2 range accessible experimentally. (We deliberately do not show the results at the smallest available $x = 5 \times 10^{-5}$ where the q -interval is too small, $0.6 \leq q \leq 0.8$, for fixing $a_2(x)$ in (4) uniquely and where moreover present measurements are not yet sufficiently accurate). Apart from the rather large values of $a_2(x)$ specific [3, 4] for the MRST01 fit, our NLO and NNLO results agree well with the experimental curvatures as calculated and presented in [2] using the H1 data [6]. Our predictions do *not* sensitively depend on the factorization scheme chosen ($\overline{\text{MS}}$ or DIS) and are, moreover, perturbative *stable* with the NNLO 3-loop results lying typically below the NLO ones, i.e. closer to present data [4]. It should be emphasized that the perturbative *stable* evolutions always result in a *positive* curvature which *increases* as x decreases.

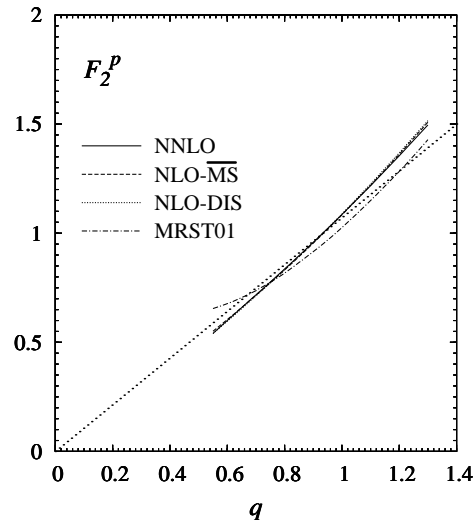


Figure 2: Predictions for $F_2^p(x, Q^2)$ at $x = 10^{-4}$ plotted versus q defined in (3).

Such unique predictions provide a sensitive

test of the range of validity of perturbative QCD! This feature is supported by the data shown in Fig. 3. Future analyses of present precision measurements in this very small- x region (typically $10^{-5} \lesssim x \lesssim 10^{-3}$) should provide additional tests of the theoretical predictions concerning the range of validity of perturbative QCD evolutions.

To conclude, perturbative NLO and NNLO QCD evolutions of parton distributions in the (very) small- x region are fully compatible with all recent high-statistics measurements of the Q^2 -dependence of $F_2^p(x, Q^2)$ in that region. The results are perturbatively stable and, furthermore, are rather insensitive to the factorization scheme chosen ($\overline{\text{MS}}$ or DIS). Therefore additional model assumptions concerning further resummations of subleading small- x logarithms are not required. A characteristic feature of perturbative QCD evolutions is a *positive* curvature $a_2(x)$ which *increases* as x decreases (cf. Fig. 3). This rather unique and perturbatively stable prediction plays a decisive role in probing the range of validity of perturbative QCD evolutions. Although present data are indicative for such a behavior, they are statistically insignificant for $x < 10^{-4}$. Future analyses of present precision measurements in the very small- x region should provide a sensitive test of the range of validity of perturbative QCD and further information concerning the detailed shapes of the gluon and sea distributions as well.

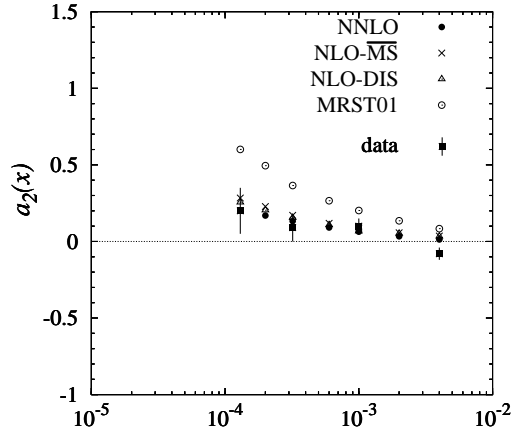


Figure 3: The curvature $a_2(x)$ as defined in (4) for the variable q -intervals in (5).

References

- [1] Slides:
<http://indico.cern.ch/contributionDisplay.py?contribId=48&sessionId=8&confId=9499>
- [2] D. Haidt, Eur. Phys. J. **C35**, 519 (2004).
- [3] M. Gluck, C. Pisano and E. Reya, Eur. Phys. J. **C40**, 515 (2005).
- [4] M. Gluck, C. Pisano and E. Reya, Eur. Phys. J. **C50**, 29 (2007).
- [5] A. Vogt, Comp. Phys. Comm. **170**, 65 (2005).
- [6] C. Adloff et al., H1 Collab., Eur. Phys. J. **C21**, 33 (2001).
- [7] C. Adloff et al., H1 Collab., Eur. Phys. J. **C30**, 1 (2003).
- [8] A.C. Benvenuti et al., BCDMS Collab., Phys. Lett. **B223**, 485 (1989); **B237**, 599 (1990).
- [9] M. Arneodo et al., NMC Collab., Nucl. Phys. **B483**, 3 (1997); **B487**, 3 (1997).
- [10] S. Forte, G. Altarelli, R.D. Ball, talk presented at **DIS 2006**, Tsukuba, Japan (April 2006), and references therein (arXiv:hep-ph/0606323).
- [11] S. Moch, J.A.M. Vermaseren, A. Vogt, Nucl. Phys. **B688**, 101 (2004).
- [12] A. Vogt, S. Moch, J.A.M. Vermaseren, Nucl. Phys. **B691**, 129 (2004).
- [13] A.D. Martin, R.G. Roberts, W.J. Stirling, R.S. Thorne, Eur. Phys. J. **C23**, 73 (2002).
- [14] J. Pumplin et al., JHEP **7**, 12 (2002).